The Visible Light Activity of the TiO_2 and $TiO_2:V^{4+}$ Photocatalyst

Regular Paper

Nguyen Minh Thuy[1,*], Duong Quoc Van[1] and Le Thi Hong Hai[2]

1 Department of Physics, Hanoi National University of Education, Hanoi, Vietnam
2 Department of Chemistry, Hanoi National University of Education, Hanoi, Vietnam
* Corresponding author: thuynm@hnue.edu.vn

Abstract TiO_2 and vanadium-doped TiO_2 nanoparticles were synthesized by using the hydrothermal method. The V doping contents are 0.0; 0.1; 0.3; 0.5; 0.7 and 0.9% molar.

The vanadium-doped TiO_2 nanoparticles have identical anatase phase with an average crystal size of 10-20nm. The oleic acid and ethanol solvents with different molar concentrations can make spherical nanograins, or stick form grains, which influence the photo activity of the materials. The absorption spectra of doped samples exhibited long-tailed absorption in the visible light region above 380nm.

The visible light photocatalytic activity was evaluated by the degradation of phenol aqueous solutions; after 360 min. under the visible irradiation, the normalized concentration of phenol decreased to 9%.

Keywords Semiconductors, Nanocrystals, Photocatalysts, Absorption, Irradiation.

1. Introduction

Titanium dioxide (TiO_2) is an important compound, the electronic structure of which continues to attract considerable experimental and theoretical attention for both fundamental interest and potential modern technological applications (see [1,2,3]). In recent years, a great deal of interest has been devoted to the photocatalytic degradation of organic water pollutants on semiconductor particles (see [4,5,6]). TiO_2 can be applicable for the decomposition of undesired compounds in air as well as waste water, solar energy conversion and the production of clean energy resources through the water splitting reaction. In particular, applications for environmental issues such as purification of waste water using natural solar light are of great practical interest. However, the application of TiO_2 as a photocatalyst for visible light-induced chemical reactions has been hampered by its large band-gap energy (3.2eV for anatase TiO_2), which requires ultraviolet (UV) light to activate and leads to the lower energy efficiency. Widening the absorption edge of TiO_2 from the UV to the visible spectral range could provide the groundwork to develop TiO_2 catalysts with visible light activity.

Many studies had been attributed to the doping of transition metals into TiO_2 to develop vis-photocatalysts, such as V, Cr, Mo, Fe (see [1,3,7]). Among the transition metal ions, vanadium ion is attractive because vanadium

doping can increase carrier lifetime and apparently also extend the absorption range of TiO2. Different methods had been chosen to prepare V-doped TiO2 catalysts, such as the sol-gel method, the metal ion-implantation method, the co-precipitation method, the hydrothermal method and so on (see [3-6]). It is promising to synthesize V-doped TiO2 powders economically and practically by using the hydrothermal method because of its low cost, effectiveness and easy execution. The performance of a TiO2 photocatalyst is strongly dependent on a number of other structural factors, such as crystal phase, as well as grain forms and the degree of crystallinity of the TiO2 particles. The technique parameters of the hydrothermal method, such as the solvent and temperatures, can directly affect the above properties of the TiO2 nanoparticles.

In this work, V–doped TiO2 nanopowders were synthesized by using the hydrothermal method. We investigated the solvent influence on morphology and particle size in the sample in order to obtain high visible photoactivity of TiO2:V nanocrystals. The solvents are water or oleic acid with ethanol, which have affected the forms and sizes of the grains in the samples.

The photodegradation of phenol (C_6H_5OH) in aqueous suspension was used as a probe reaction to evaluate the photocatalytic activity.

As shown in previous works, the metal doping in nanosize TiO2 has no identify effect on the photocatalystic activity of titana: ref. [7] illustrated that the visible light photoactivity of doped vanadium is lower than that of undoped titania prepared by the solution combustion method. However ref. [5], using the hydrothermal method, obtained an effectively improved reaction rate for the degradation of isobutanol by small amounts of vanadium doping into TiO2. The photocatalyst of doped nanosize titana is strongly related to the sample preparation method [4,5,7]. In our previous work [8], we found that by using the hydrothermal method the 0.5%V-doped TiO2 anatase nanocrystals have the highest visible light activity; undoped TiO2 has photocatalyst only under UV-radiative excitation. This result is in good agreement with [9,10] in methyl orange photocatalytic degradation. However, the sample prepared with the water solvent had a low degradation rate (after 360 min. of visible irradiation, the normalized concentration of phenol decreased to 30%). In this work we intend to improve the grain form and size by changing the polarity of the solvent. Oleic acid ($C_{17}H_{33}COOH$) and ethanol (C_2H_5OH) solvent can be used for this. The different ratios of oleic acid/ethanol were made to control the morphology and grain form in the samples, hence their photocatalystic activity can be improved. After 360 min. of visible irradiation with TiO2:V nanoparticle treatment, the normalized concentration of phenol decreased to 9% and the concentration of phenol decreased to 0.003mg/l, which is less than the allowable phenol value on industrial waste water by discharge standards. The visible light photocatalystic activity of V-doped TiO2 suggested an application for an environmental treatment of waste water.

2. Experiment

The used chemicals were TiCl4, acid citric (CA), NH4NO3, NH3 10%, V2O5/HCl 0.03M, oleic acid (OA) $C_{17}H_{33}COOH$ (pKa=9.85 [11]) and C_2H_5OH. All chemicals were of analytical reagent grade. Pure titanium catalyst was prepared using the hydrothermal method with the following procedure: firstly 3.0ml TiCl4 was added drop by drop to 100ml of solvent (distilled water or OA), which was continuously stirred for 20 min. Afterwards, ammonia aqueous solution NH3 (25%) was added to adjust the pH value to 7-8, and then stirred for 30 min. Then the mixture was transferred into an autoclave and kept at 200^{0}C for 5h. After centrifugation and washing, the samples were dried in the air.

A series of V-doped TiO2 hydrosols were prepared by changing the V/Ti ratio. The vanadium doping content was calculated by the following equation:

$$\%V = n_V/(n_V + n_{Ti})$$

where n_V and n_{Ti} were the mole of vanadium and titanium, respectively.

The V doping contents are 0.0; 0.1; 0.3; 0.5; 0.7 and 0.9 molar %.

For studying the influence of the solvents, we chose the sample TiO2:0.5%V. The different proportions of the TiCl4: OA: C_2H_5OH are 1:4:20; 1:5:20; 1:6:20 and 1:8:20. We name the obtained samples as T^{1420}_5; T^{1520}_5; T^{1620}_5 and T^{1820}_5, respectively.

The structure and crystalline characters were analysed by X-ray diffraction (XRD) SIEMENS D5005, selected area electron diffraction (SEAD), and by Raman scattering measurements with LABRAM micro-Raman spectroscopy. X-ray photoelectron spectroscopy (XPS) measurements were performed in a commercial Microlab 350 XPS system equipped with an Al Kα source, in a UHV chamber (~10^{-9} Torr) with a 60° take off angle.

The morphology was investigated by using a scanning electron microscope (SEM), transmission electron microscope (TEM) and a high resolution TEM (HR-TEM). Absorption measurements were obtained with a JASCO V-670 spectrometer.

The photocatalytic activity of samples was evaluated by degradation of phenol (C_6H_5OH) diluted in water. All phenol-diluted water samples were prepared as follows: 80ml phenol solution (5.10^{-5} mol/l) was stirred in dark conditions. Then 200mg of TiO_2–based photocatalysts was added to the phenol solution and the mixture was stirred for 60 min. under dark conditions. Next visible light irradiation was carried out using a 100W Wolfram lamp with an emission spectral range from 400 to 800nm. The progress of the reactions was monitored by high performance liquid chromatography – HPLC for 360 min.

3. Result and discussions

3.1 Sample characterization

Fig.1 presented the XRD patterns of V doping TiO_2 powders. For all doping samples, the XRD patterns show only anatase TiO_2 peaks.
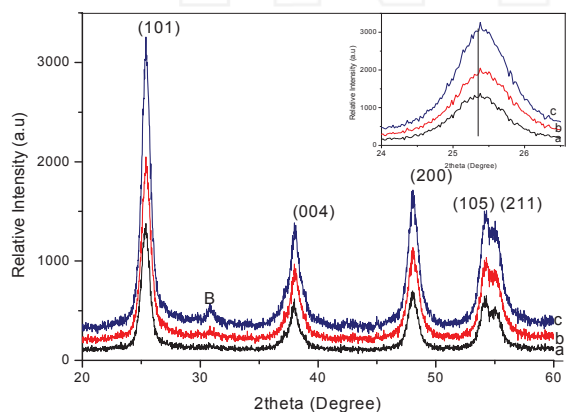

Figure 1. The XRD patterns of TiO_2 (a); 0.3% (b) and 0.5% (c) V-doped samples. The inset shows (101) peak in detail.

The average crystallite size was calculated using the Scherer's formula giving a value of about 10nm, which is in good agreement with the value determined by TEM. In the XRD patterns, there is one light peak (B) at 31.2 and its intensity is increased with the V doping content. This XRD peak may be related to the existence of the brookite TiO_2 in the samples. A more detailed picture of the (101) XRD peak (in the inset) shows a systematically peak-position shift to the higher 2Theta with the increasing vanadium doping concentration, which indicates vanadium incorporation in the anatase TiO_2.

Transmission electron microscopy (TEM) was used to examine the crystallite/particle size, the crystallinity and morphology of the samples. TEM observation (fig.2a) revealed that the prepared samples consisted of particles of 10-30 nm in size. The selected area electron diffraction (SEAD) pattern (fig.2a-insert) shows the three diffraction rings, which are perfectly indexed to the same position as those from anatase TiO_2. Moreover, the HR-TEM images (fig.2b) show the regular structure in the grain, which is

selected for analysing by Gatan digital micrograph (DM) 1.5. Fig.2c is an image of the inverse fast Fourier transform (IFFT) of the selected regular region in fig.2b obtained by Gatan DM (see [12]). Fig.2d is the IFFT profile of the selected region in fig.2c after mask application, which shows the spacing of the observed lattice plane is ca. 0.354nm. This value is consistent with the separation of (101) planes of TiO_2 anatase.
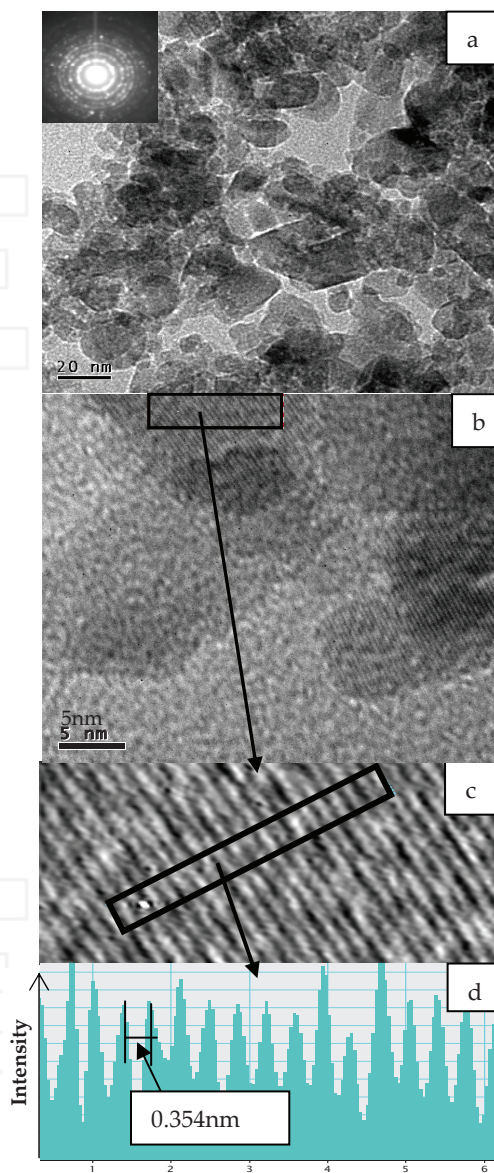

Figure 2. TEM (a); SEAD (a-inset) and HR- TEM (b) images of TiO_2:0.5%V^{4+} nanoparticles; (c) is the image of inverse fast Fourier transform of the selected region in (b); and (d) is the profile of IFFT of the selected region in (c), obtained from Gatan DM analysing.

Fig.3 presents the Raman scattering patterns of undoped TiO_2 and V-doped TiO_2. In general, the Raman spectrum of TiO_2 is characterized by a strong band at 146cm^{-1} (vibration mode Eg), three bands at 396, 517 and 639 cm^{-1} (modes Eg, B1g/A1g and Eg), and a weak band at 196cm^{-1} (mode Eg).
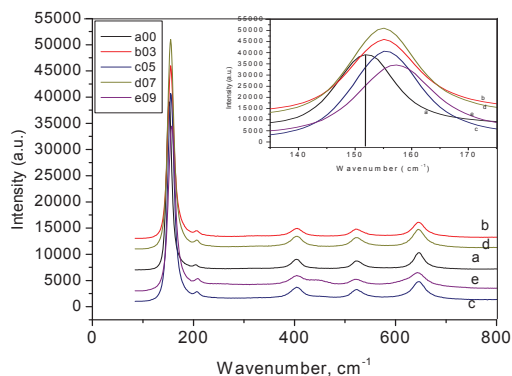
Figure 3. The Raman spectra of TiO₂ (a) and V-doped TiO₂ (b-e) and their detailed Eg-146cm⁻¹ Raman peaks (insert).

The observed spectrum showed that the nanoparticles were complete anatase phase. The typical peaks of nano anatase TiO₂ are light blue-shift (about 5 cm⁻¹) from that of the bulk sample, which can be attributed to the quantum size effect that comes from the small particle size.

Detailed Eg-146cm⁻¹ Raman peaks of undoped TiO₂ and V-doped TiO₂ are presented in fig.3 - insert. Compared with the undoped sample, the Eg-vibrations at 146 and 197 cm⁻¹ presented a light blue-shift after V doping, which indicated the vanadium incorporation into the TiO₂ host lattice. All peaks became wide and slightly unsymmetrical after V doping. In this study the blue shift can be ascribed to the TiO₂ lattice structure distortion due to V doping. This blue shift can be also partly attributed to the oxygen defects (see [9]). The lattice structure distortion due to V doping can also be seen in the absorption spectra.
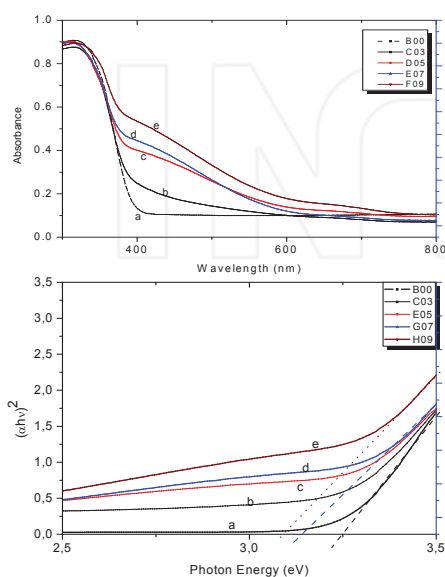

Figure 4. UV-Vis absorption spectra of TiO₂ (a) and V-doped TiO₂ (b-e).

The optical absorption spectra of TiO₂ and V-doped TiO₂ samples are presented in fig.4. Pure TiO₂ (curve a)

exhibited the absorption edge at around 3.2 eV (380nm), which corresponded to the band gap of anatase type of TiO₂. The V-doped TiO₂ exhibited the red-shift of the band edge and the long-tailed absorption in the visible light above 380nm. Compared with the spectrum of undoped TiO₂ (curve a-00), the band edges are shifted systematically toward smaller energy in the doped samples. V dopants in TiO₂ host have been determined to preferentially substitute Ti⁺⁴ ions, where one V and six Os constitute a local symmetry D2d [13,14]. The red absorption shift is attributed to the charge transfer between valence bands to the t₂g level of vanadium (splitting of 3d orbitals of V⁺⁴ in octahedral TiO₂ host [10]), which lies just below the conduction band [10,13].

The tailing of the absorption band in the doped samples can be assigned to the charge-transfer transition from the d orbital of V⁴⁺ to the conduction band of TiO₂ (see [6,7]). The weak absorption band around 2.5eV (650-700nm) can be due to the d-d transitions of V3d electrons. Besides the d-d transition, the gap states introduced by V doping were another important reason for the visible light absorption (see [7]). According to ref. [9], the weak absorption band tail of undoped TiO₂ comes from the momentary localization of excitons due to the phonon interaction, and the strong band tail of the V-doped TiO₂ nanoparticles mainly contributed to the impurities and lattice disorder, which also indicated the formation of gap states, in accordance with the result of the calculation in [13,15]. In the present work, we suppose that the strong band tail in the visible light of V doping TiO₂ nanopowders is related to the d-d transition of V⁴⁺ in the host TiO₂ and also to the lattice distortion. The evidence of the V⁴⁺ in host TiO₂ and lattice structure distortion due to V doping can also be seen by the XPS spectra. Fig 5.a. shows the Ti 2p core-level spectra of undoped and vanadium-doped samples. As is well-known, the Ti 2p peak splits into Ti 2p₃/₂ (~459 eV) and Ti 2p₁/₂ (~464.5 eV) due to the self-orbital coupling effect. For the undoped sample, these peaks were symmetrical, indicating that Ti⁺⁴ were mainly presented in the undoped sample. The Ti 2p peak became wide and unsymmetrical after V doping, which may be related to more oxygen defects after V doping (it can lead to Ti₂O₃ formation). Fig 5.b illustrates the O 1s core level XPS spectra of undoped and vanadium-doped samples. The O 1s peak (~ 530 to 532 eV for undoped TiO₂) is often believed to be composed of several different oxygen species, such as Ti-O bonds in TiO₂ or Ti₂O₃, hydroxyl groups, C-O bonds and adsorbed H₂O. In the XPS spectra of the doped sample, this peak is broadened, which can be analysed to three components (see fig.5.c and d): (i) the main peak (~ 530 eV for undoped and ~ 531.5÷ 533 eV for doped samples) could be ascribed to the lattice oxygen in TiO₂ (Ti-O-Ti); (ii) the light shoulder at 533÷534 eV could be associated to surface hydroxyl (Ti-OH) groups ([9,16]); and (iii) for the doping samples there could be another peak at ~534 eV of

V-O groups (see [9]). The last (V-O) peak is increased with the doping effect. The V doping led to the O 1s peak shifting to higher binding energy, which indicated the O valence increase [9].
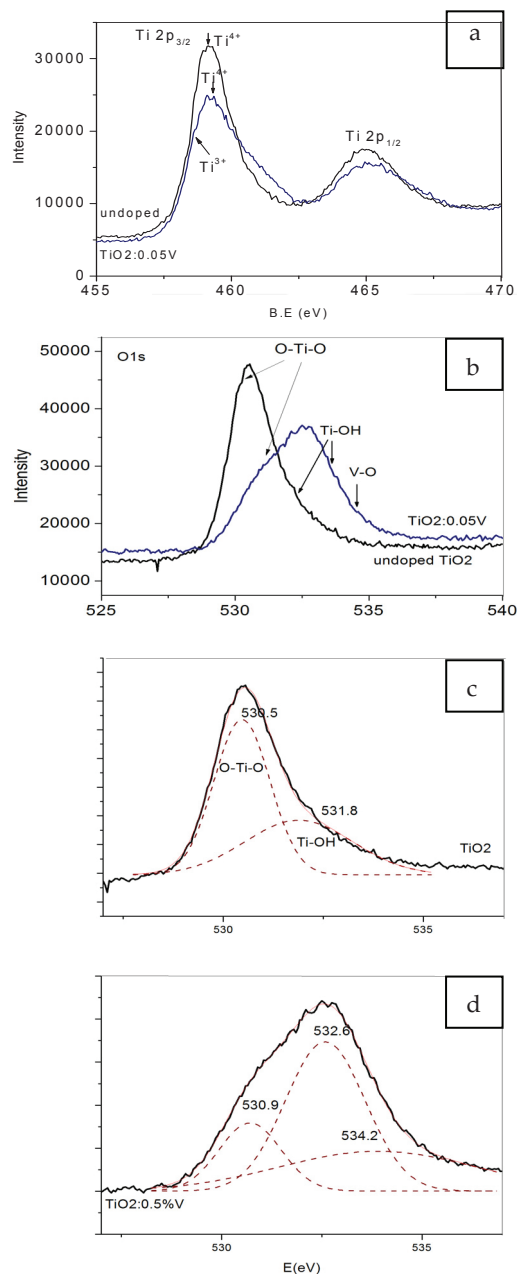

Figure 5. The Ti 2p (a) and O 1s (b) XPS spectra of undoped and 0.05 vanadium-doped samples; The Gaussian fits of O 1s of pure (c) and 0.05V-doped TiO2 (d).

3.2 Influence of the solvent on the structure properties of samples

Figure 6 presents TEM images of 0.5%V-doped TiO_2 with different solvents. In this work we used oleic acid (OA), pKa=9.85 [11] and ethanol solvent samples to study the solvent effect. The different proportions of the $TiCl_4$: $OA:C_2H_5OH$ are 1:4:20; 1:5:20; 1:6:20 and 1:8:20. We named the obtained samples as $T^{1420}5$; $T^{1520}5$; $T^{1620}5$ and $T^{1820}5$, respectively.
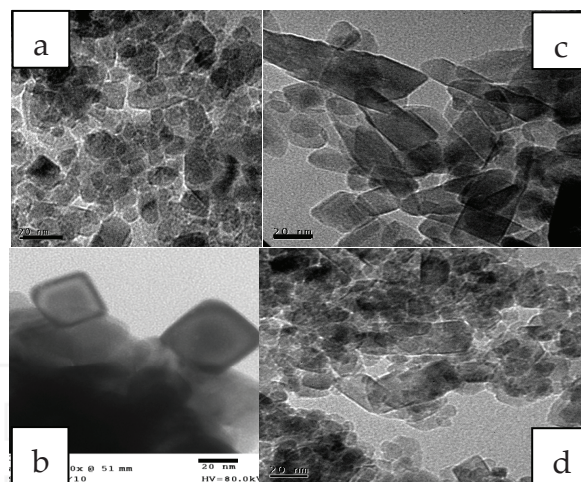

Figure 6. TEM images of the TiO_2:0.5% V^{4+} with different OA-solvent: the ratios of $TiCl_4$: OA: C_2H_5OH are 1:4:20 (a); 1:5:20 (b); 1:6:20 (c) and 1:8:20 (d).

Figure 6 present TEM images of $T^{1420}5$ (a), $T^{1520}5$ (b), $T^{1620}5$ (c) and $T^{1820}5$ (d), respectively. The TEM images showed that the different OA solvents had an influence on the morphology of the samples. The samples have random spheroid-like (a,d), cubic-like (b) or similar rod-like (c) morphologies. The grain size in the samples is also related to the concentration of the solvent. The proportions $TiCl_4$: OA: C_2H_5OH of solvents of 1:8:20 (d) led to the smallest grain size, which is 10nm. This result may be related to the polarity of the solvent. As is well-known, OA ($C_{17}H_{33}COO^-$) consists from two parts: the polar part (COO^-)-hydrophilous and the other non-polar part ($C_{17}H_{33}^-$)- hydrophobic. Due to the non-polar part, the polarity of the OA solvent is lower than that of water; hence, the grain formation can be controlled by changing the ratio of $C_{17}H_{33} COO^-/C_2H_5OH$. The morphology and grain form in the sample related very closely to the photocatalytic activity of the sample.

3.3 Photocatalytic activity measurement

The photocatalystic degradation of phenol has been chosen as a model reaction to evaluate the photocatalystic activities of the obtained TiO2-based catalysts.

Phenol (C_6H_5OH) is a common chemical that is used extensively in a variety of industrial applications. Phenol was selected as a model pollutant for the photocatalytic oxidation experiments. All phenol-diluted water samples were prepared as follows: 80ml (C_6H_5OH) solution (5.10^{-5} mol/l) was stirred in dark conditions. Then 200mg of TiO2-based photocatalysts was added to the phenol solution and the mixture was stirred for 60 min. under dark conditions. Next, visible light irradiation was carried

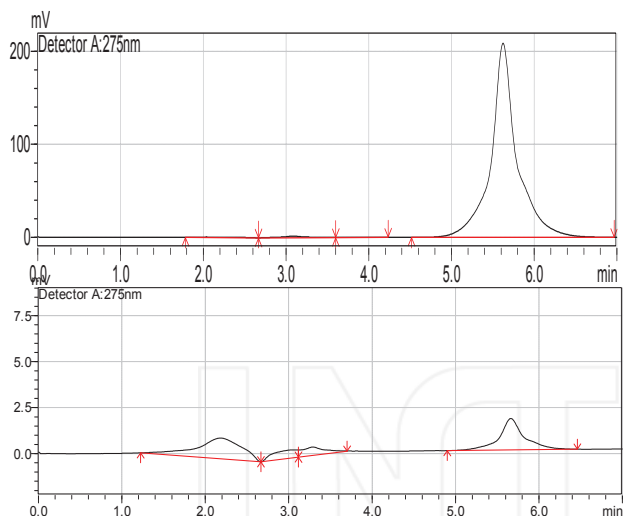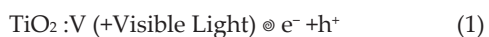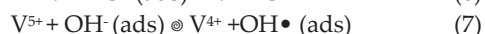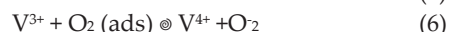out using a 100W Wolfram lamp with an emission spectral range from 400 to 800nm.

Figure 7. Chromatographs of phenol degradation using TiO$_2$:0,5%V under vis-irradiation at 0 (over) and 360 min. (below).

Fig.7 presents the chromatographs of the phenol degradation of phenol pollution water using TiO$_2$:0.5%V as photocatalysts, which were recorded by HPLC at 0 and 360 min. after visible irradiation. By calculating and comparing the squares of phenol peaks (at $t_{rent.}$=5.6 min.) in the chromatographs, we obtained the phenol degradation rate (C/Co) in the photocatalytic process.

In our work we found that undoped TiO$_2$ has photocatalyst only under UV-radiative excitation [8]. By using the hydrothermal method, the optimal vanadium doping concentration for visible light photocatalyst is 0.5% molar. The photodegradation of phenol using TiO$_2$:V nanocrystals can be explained as follows. The undoped TiO$_2$ anatase has only a UV optical band gap (3,2eV), hence it cannot be excited under visible irradiation. The excitation behaviour of V–TiO$_2$ under visible irradiation might be related to V 3d orbital. Due to the fact that the t_{2g} level of V 3d orbital lies a little below the conduction band edge of TiO$_2$ [10,13], electrons can be excited from the valence band of TiO$_2$ to the t_{2g} level of V 3d orbital under visible light irradiation (Eqs.(1)), and further migrate to adsorbed O$_2$ to form O$^-_2$. Meanwhile, holes migrate to the surface hydroxyl group to produce hydroxyl radicals (OH•). Both of O$_2^-$ and OH• can further degrade phenol. Thus, phenol was degraded under visible light irradiation. The photocatalytic degradation processes can be described by Eqs. (1)–(7). V^{4+} ions, acting as both electron and hole traps, can turn into V^{3+} and V^{5+} ions by trapping photogenerated electrons and holes, respectively (Eqs. (2) and (3)).

$$TiO_2 :V \text{ (+Visible Light)} \rightarrow e^- +h^+ \qquad (1)$$
$$V^{4+} +e^- \rightarrow V^{3+} \qquad (2)$$
$$V^{4+} +h^+ \rightarrow V^{5+} \qquad (3)$$

Then, the trapped electrons and holes are released (Eqs. (4) and (5)) and migrate to the surface of TiO$_2$. By accepting an electron, the adsorbed O$_2$ on the surface of TiO$_2$ is reduced to O$_2^-$ (Eq. (6)), while the surface hydroxyl group translates into hydroxyl radical (OH•) by accepting a hole (Eq. (7)).

$$V^{3+} \rightarrow V^{4+} +e^- \qquad (4)$$
$$V^{5+} \rightarrow V^{4+} +h^+ \qquad (5)$$
$$V^{3+} + O_2 \text{ (ads)} \rightarrow V^{4+} +O_2^- \qquad (6)$$
$$V^{5+}+ OH^- \text{ (ads)} \rightarrow V^{4+} +OH• \text{ (ads)} \qquad (7)$$

So, the incorporation of V^{4+} ions in TiO$_2$ lattice can restrain the recombination rate of photogenerated electrons and holes, enhancing the photocatalytic activity of TiO$_2$. However, too high a V concentration (more than 0.5%) can lead to a decrease of photocatalytic activity. This trend can be related to several effects: (i) if the concentration of V^{4+} ions is too high, they can become the recombination centres of photogenerated electrons and holes; (ii) the specific surface area decreases with the increase of V concentration which is unfavourable for obtaining high photocatalytic activity.
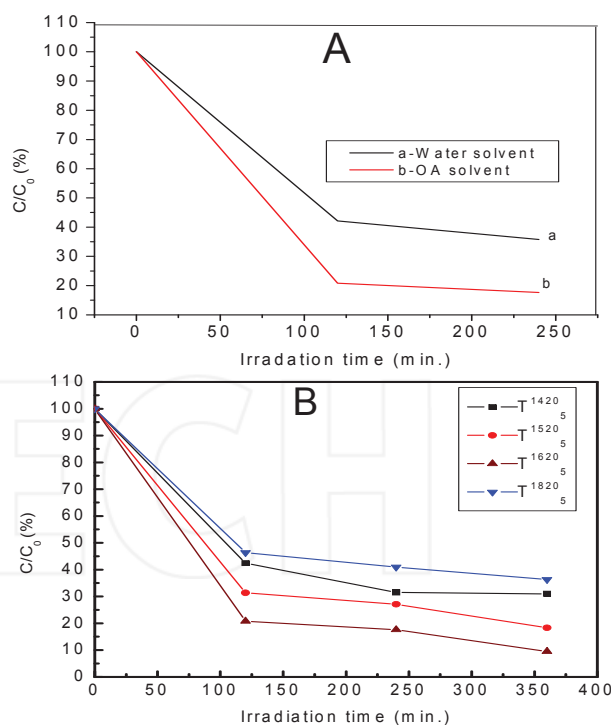

Figure 8. Photocatalytic phenol degradation curves of the 0.5% V-doped TiO$_2$ photocatalyst prepared with different solvents.

Fig.8 describes the photocatalystic activity of the 0.5%V-doped TiO$_2$ samples prepared with different solvents. One can see that the sample prepared with the OA solvent (b curve in fig.8A) exhibited higher photocatalystic activity than that with the water solvent. This trend may be related to the lower polarity of the OA

solvent; hence the grain size of OA samples is smaller. Among the samples prepared with the OA and ethanol solvent (fig.8B), the sample with the proportions $TiCl_4$: OA: C_2H_5OH of 1:6:20 had the best photocatalystic activity. After 360 min. irradiation, the current normalized phenol concentration decreased to 9.0%. This result may be related to the rod-like morphology of the sample, which is shown in the fig.6c. The rod-like morphology of the samples can lead to increasing specific surface areas, hence improving their photoactivity.

4. Conclusions

The pure and vanadium doping TiO_2 nanocrystals were successfully prepared by using hydrothermal methods with different solvents. The doping V concentration was in a range from 0.1% to 0.9%. All obtained samples were single anatase crystal phase. The average crystal size was about 10-20nm.

The vanadium-doped samples exhibited long-tailed absorption in the visible light above 380nm. This can be related to the charge-transfer transitions from the d-d orbital of V to the conduction band of TiO_2 and lattice disorder.

The grain form and size are dependent on the polarity of the solvent. Oleic acid and ethanol can be used for the solvent polarity controller; hence, the photoactivity properties of the samples can be improved.

The phenol-degradation measurements under visible light showed that the 0.5% vanadium-doped sample with the proportions $TiCl_4$: OA: C_2H_5OH of 1:6:20 had the best photocatalystic activity. After 360 min. visible light irradiation, the current normalized phenol concentration decreased to 9% (the concentration of phenol decreased to 0.003mg/l, which is less than the allowable phenol value on industrial waste water by discharge standards).

The visible light photocatalystic of the material suggested an application for an environmental treatment of waste water.

5. Acknowledgements

6. References

[1] W.Choi, A.Termin and M.R. Hoffmann, "The Role of Metal Ion Dopants in Quantum-Sized TiO_2: Correlation between Photoreactivity and Charge Carrier Recombination Dynamics", *J.Phys. Chem.* **98** (1994)13669.

[2] E.Graugnard, J.S.King, S.Jain, C.J.Summers, Y.Zhang-Williams and I.C.Khoo, "Electric field tuning of the Bragg peak in large-pore TiO_2 inverse shell opals", *Phys.Rev.B* 72 (2005) 233105.

[3] N.Van Duy, N.Van Hieu, P.Thanh Huy, N.Duc Chien, M.Thamilselvan, J.Yi, "Mixed SnO_2/TiO_2 included with carbon nanotubes for gas-sensing application", *Physica E: Low-dimensional Systems and Nanostructures*, V.41, Iss.2 (2008)pp. 258-263.

[4] L.Wang and T.Egerton, "The effect of transition metal on the optical properties and photoactivity of nanoparticulate titanium dioxide", *J. of Materials Science Research* v.1, N.4, 2012.

[5] T.Kamegawa, J.Sonoda, K.Sugimura, K.Mori, H.Ymashita, "Degradation of isobutanol diluted in water over visible light sensitive vanadium doped TiO_2 photocatalyst", *Journal of Alloys and Compounds* 486, (2009) pp.685-688.

[6] S.Liu, T.Xie, Z.Chen, J.Wu, "Highly active V–TiO_2 for photocatalytic degradation of methyl orange", *Applied Surface Science* 255, (2009) pp.8587–8592.

[7] K.Nagaveni, M.S. Hegde, G. Madras, "Structure and Photocatalytic Activity of $Ti_{1-x}M_xO_2$ (M = W, V, Ce, Zr, Fe, and Cu) Synthesized by Solution Combustion Method", *J. Phys. Chem. B*.108 (2004) pp.20204.

[8] N.M.Thuy, L.T.H.Hai, T.M.Duc and N.T.H.Thanh, "A visible light activity of TiO_2 based photocatalysts", *The 5th International Workshop on Advanced Materials Science and Nanotechnology (IWAMSN2010) - Hanoi, Vietnam* – Nov. 09-12, 2010.

[9] B. Liu, X.Wang, G.Cai, L.Wen, Y.Song, X.Zhao, "Low temperature fabrication of V – doped TiO_2 nanoparticles, structure and photocatalytic studies", *J. of Hazardous Materials* 169 (2009) pp. 1112-1118.

[10] B.Tian and C.Li, "Flame sprayed V-doped TiO_2 nanoparticles with enhanced photocatalytic activity under visible light irradiation", Chem. Engineering J. 2009; 151; 220-7.

[11] J.R.Kanicky and D.O.Shah, "Effect of Degree, Type, and Position of Unsaturation on the pKa of Long-Chain Fatty Acids", *Journal of Colloid and Interface Science* 256 (2002), 201–207

[12] http://www.gatan.com/imaging/dig_micrograph.php

[13] Y.Wang and D.J. Doren, "Electronic structures of V-doped anatase TiO_2", *Solid state Commun.* 136 (2005) pp. 142-146.

[14] Y.Hwu, Y.D.Yao, N.F.Cheng, C.Y.Tung and H.M.Lin, "X-ray absorption of nanocrystal TiO_2", *Nanostructured Materials*, V.9, I1-8 (1997) 355-358.

www.intechopen.com

Nguyen Minh Thuy, Duong Quoc Van and Le Thi Hong Hai: 7
The Visible Light Activity of the TiO_2 and TiO_2:V^{4+} Photocatalyst

[15] H.Tang, F.Levy, H. Berger and P.E. Schmid, "Urbach tail of anatase TiO_2", *Phys.Rev. B* 52 (1995) pp. 7771-7774.

[16] J.Zhu, J.Yang, Z.-F.Bian, J.Ren, Y.-M.Liu, Y.Cao, H.-X.Li, H.-Y.He, K.-N.Fan, "Nanocrystalline anatase TiO_2 photocatalysts prepared via a facile low temperature nonhydrotic sol-gel reaction of $TiCl_4$ and benzyl alcohol.", *Appl. Catal. B: Environmental* 76 (2007) pp. 82-91.